Connexin36 contributes to INS-1E cells survival through modulation of cytokine-induced oxidative stress, ER stress and AMPK activity

F Allagnat[1], P Klee[2], AK Cardozo[3], P Meda[2] and J-A Haefliger*,[1]

Cell-to-cell communication mediated by gap junctions made of Connexin36 (Cx36) contributes to pancreatic β-cell function. We have recently demonstrated that Cx36 also supports β-cell survival by a still unclear mechanism. Using specific Cx36 siRNAs or adenoviral vectors, we now show that Cx36 downregulation promotes apoptosis in INS-1E cells exposed to the pro-inflammatory cytokines (IL-1β, TNF-α and IFN-γ) involved at the onset of type 1 diabetes, whereas Cx36 overexpression protects against this effect. Cx36 overexpression also protects INS-1E cells against endoplasmic reticulum (ER) stress-mediated apoptosis, and alleviates the cytokine-induced production of reactive oxygen species, the depletion of the ER Ca^{2+} stores, the CHOP overexpression and the degradation of the anti-apoptotic protein Bcl-2 and Mcl-1. We further show that cytokines activate the AMP-dependent protein kinase (AMPK) in a NO-dependent and ER-stress-dependent manner and that AMPK inhibits Cx36 expression. Altogether, the data suggest that Cx36 is involved in Ca^{2+} homeostasis within the ER and that Cx36 expression is downregulated following ER stress and subsequent AMPK activation. As a result, cytokine-induced Cx36 downregulation elicits a positive feedback loop that amplifies ER stress and AMPK activation, leading to further Cx36 downregulation. The data reveal that Cx36 plays a central role in the oxidative stress and ER stress induced by cytokines and the subsequent regulation of AMPK activity, which in turn controls Cx36 expression and mitochondria-dependent apoptosis of insulin-producing cells.
Cell Death and Differentiation (2013) **20,** 1742–1752; doi:10.1038/cdd.2013.134; published online 4 October 2013

The fine-tuning of insulin secretion in response to nutrient stimulation requires a tight coordination of pancreatic β-cells, which is achieved by multiple mechanisms.[1,2] The direct intercellular communication provided by connexin-made gap junctions is key to integrate individual cells into coordinated multicellular units.[1,2] Gap junction-mediated intercellular communication also modulates apoptosis in a variety of systems, even though the effect may be anti- or pro-apoptotic, depending on the connexin isoform and the cell type.[3] We recently reported that mice lacking Connexin36 (Cx36), the sole connexin expressed in β-cells,[1,2] are sensitized to cytotoxic drugs and cytokines, whereas mice overexpressing Cx36 in β-cells are more resistant to these insults.[4] However, the molecular mechanism of this protection remains to be established.

Type 1 diabetes (T1D) originates from the autoimmune destruction of pancreatic β-cells, mostly through apoptosis induced by pro-inflammatory Th1 cytokines (interleukine-1 beta (IL-1β), tumor necrosis factor alpha (TNF-α) and interferon gamma (IFN-γ)) and other pro-apoptotic mediators

released by or expressed at the surface of the immune cells infiltrating the islets of Langerhans.[5] Increasing evidence suggests a combined involvement of endoplasmic reticulum (ER) stress, oxidative stress and mitochondrial dysfunction in the induction of β-cell apoptosis,[6–8] as per the so-called intrinsic pathway.[9] This pathway is characterized by the permeabilization of the outer mitochondrial membrane, leading to the leakage of mitochondrial proteins such as cytochrome c, which, after association with cytosolic proteins, activate the downstream caspases that ultimately trigger apoptosis.[10,11] We recently showed that the C/EBP homologous protein (CHOP) and the anti-apoptotic proteins Bcl-2 and Mcl-1 are key to the regulation of this pathway in β-cells.[12]

Here, we have investigated the molecular mechanism linking Cx36 signaling to the intrinsic pathway. We show that exposure to cytokines, particularly IL-1β, reduces Cx36 expression in insulin-secreting cell lines and primary β-cells. This effect is mediated by the Ca^{2+}-dependent activation of the AMP-activated protein kinase (AMPK), a metabolic stress-sensing protein kinase responsible for coordinating
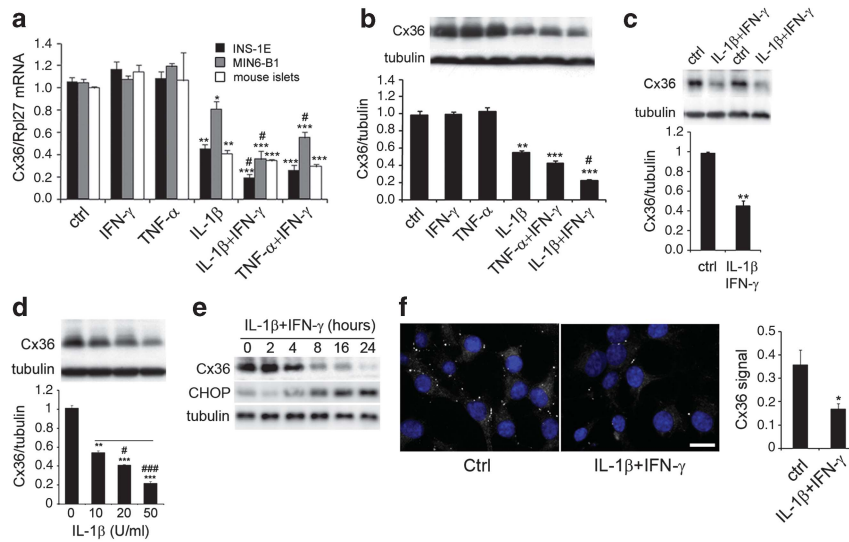
Figure 1 Pro-inflammatory cytokines downregulate Cx36 in β-cells. (**a**) Cx36 over Rpl27 transcript levels in INS-1E cells, MIN6-B1 cells and primary mouse islets cultured for 24 h in the presence or absence (ctrl) of IL-1β (10 U/ml), TNF-α (1000 U/ml) and/or IFN-γ (100 U/ml), alone or in combination as indicated. Data are mean ± S.E.M. of 4–6 independent experiments. (**b**) Upper panel: representative western blot analysis of Cx36 and tubulin in INS-1E cells cultured for 24 h in the presence or absence (ctrl) of IL-1β, TNF-α and/or IFN-γ, alone or in combinations. Lower panel: quantitative assessment of five independent experiments. (**c**) Western blot analysis and quantitative assessment of Cx36 over tubulin in primary rat islets cultured for 24 h in the presence of IL-1β + IFN-γ. $n = 4$. (**d**) Western blot analyses and quantitative assessment of Cx36 over tubulin in INS-1E cells cultured for 24 h in the presence of increasing concentrations of IL-1β as indicated. (**e**) Time-course analysis of Cx36, CHOP and tubulin in INS-1E cells cultured in the presence of IL-1β + IFN-γ (representative of three independent experiments). (**f**) Cx36 immunolabeling dots (white dots) and DAPI (nuclear staining in blue) of INS-1E cells cultured in the presence of IL-1β + IFN-γ for 24 h. White bar: 10 μm. *$P<0.05$; **$P<0.01$; ***$P<0.001$ versus ctrl #$P<0.05$; ###$P<0.0001$ versus IL-1β or TNF-α alone

metabolism and energy demands.[13] In turn, AMPK inhibits the CREB-regulated transcription coactivator 2 (Crtc2), leading to a decrease in the promoter activity of the Cx36 gene *GJD2*. We further document that low levels of Cx36 increase the effects of ER stress and AMPK activation, leading to a further downregulation of Cx36 and enhanced β-cell apoptosis. The data provide evidence that Cx36 modulates ER Ca^{2+} homeostasis and molecular components of the intrinsic mitochondrial pathway of apoptosis, which ultimately regulate the death of insulin-producing β-cells.

Results

Cytokines reduce Cx36 expression and function in insulin-producing cells and primary mouse islets. To evaluate the effect of the pro-inflammatory cytokines on Cx36 expression, insulin-producing cells and primary mouse islets were treated with IL-1β, TNF-α and IFN-γ, alone or in combination. Supplementary Figure S1 shows that a 24-h exposure to 1000 U/ml TNF-α or 100 U/ml IFN-γ did not affect insulin-secreting cells viability. In contrast, 10 U/ml IL-1β significantly increased insulin-secreting cells apoptosis in both primary islets and insulin-producing cell lines (Supplementary Figure S1). The combination of TNF-α and IFN-γ significantly decreased viability levels in all models, and the addition of IFN-γ potentiated the negative effect of IL-1β (Supplementary Figure S1). We then studied the Cx36 mRNA regulation in the same conditions and observed that Cx36 mRNA levels are closely correlated with cell survival in all models (Figure 1a). TNF-α + IFN-γ also decreased Cx36 protein levels, and IFN-γ potentiated the effect of IL-1β alone,

Table 1 Dye coupling of INS-1E cells after a 24 h exposure to either IL-1β or metformin

Condition	Extent of coupling[a]	Incidence of coupling[b]	Coupling index[c](a.u.)	Number of microinjections
Control	2.5 ± 0.2	28 (65.1)	162.1	43
IL-1β	1.5 ± 0.1***	12 (41.4)*	60.0	29
Metformin	1.4 ± 0.1***	8 (32.0)**	43.5	25

[a]Data are mean ± S.E.M. values of the number of cells featuring labeling by Lucifer yellow, in the number of microinjections indicated in the right column. ***$P<0.001$ compared with the value in control cells, as evaluated by ANOVA.
[b]Number and (proportion) of injections resulting in the intercellular transfer of the dye. *$P<0.04$, **$P<0.008$ versus control as evaluated by the non parametric χ^2-test.
[c]Given by average extent χ percentage of coupling.

both in INS-1E cells and primary mouse islets (Figures 1b and c). IL-1β decreased the protein levels of Cx36 in a dose-dependent manner (Figure 1d). Time-course experiments further revealed that IL-1β + IFN-γ time-dependently decreased the Cx36 protein expression in INS-1E cells (Figure 1e). Consistently, a 24-h cytokine treatment decreased the typical punctate immunostaining of Cx36 in INS-1E cells (Figure 1f). These conditions also resulted in a significant decrease in both the extent and the incidence of INS-1E coupling, as evaluated by the intercellular exchange of the gap junction tracer Lucifer Yellow (Table 1).

The levels of Cx36 influence apoptosis and the production of reactive oxygen and nitrogen species in INS-1E cells. To investigate the involvement of Cx36 in cytokine-induced apoptosis, we used siRNA and adenoviral
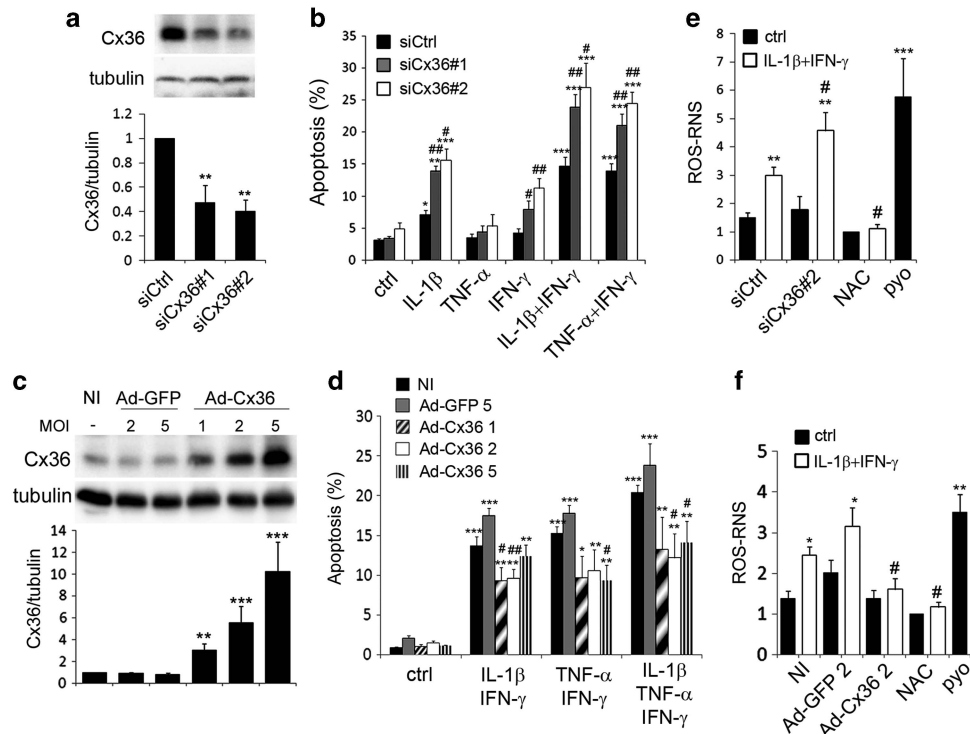
Figure 2 Changes in Cx36 expression modulate the cytokine-induced ROS–RNS production and apoptosis of INS-1E cells. (**a**, **b** and **e**) INS-1E cells were transfected with a control siRNA (siCtrl) or two different Cx36 siRNAs (siCx36#1 and #2). (**c**, **d** and **f**) INS-1E cells were infected or not (NI) with a control adenovirus (Ad-GFP) or a rat Cx36 adenovirus (Ad-Cx36) at various multiplicity of infection (MOI), as indicated. (**a** and **c**) Western blot analysis of Cx36 over tubulin levels. (**b** and **d**) Prevalence of apoptosis was evaluated by Hoechst–PI staining in cells treated or not (ctrl) for 24 h with IL-1β, TNF-α and/or IFN-γ, alone or in combination, as indicated. (**e** and **f**) ROS–RNS production was evaluated in live cells treated for 15 h with IL-1β + IFN-γ, together or not with 1mM N-acetyl cystein (NAC), or in cells treated for 30 min with 200 μM pyocyanin (pyo). *$P < 0.05$, **$P < 0.01$, ***$P < 0.001$ versus ctrl. #$P < 0.05$, ##$P < 0.01$ versus siCtrl-transfected or NI condition

transfer strategies to modulate its content. Two distinct siRNAs targeting Cx36 mRNA induced a 60% decrease in Cx36 mRNA and protein levels in INS-1E cells (Supplementary Figures S2 and 3a). This knockdown did not alter the apoptosis of control or TNF-α-treated INS-1E cells (Figure 2b) but significantly increased the apoptosis induced by IL-1β, TNF-α + IFN-γ or IL-1β + IFN-γ, and sensitized the INS-1E cells to IFN-γ alone (Figure 2b). Conversely, the adenoviral-mediated overexpression of Cx36 (Figure 2c) significantly reduced the apoptosis induced by TNF-α + IFN-γ, IL-1β + IFN-γ or a combination of the three cytokines (Figure 2d).

A 15-h IL-1β + IFN-γ treatment did not trigger the formation of superoxide species (data not shown), but stimulated the production of ROS–RNS, which was fully inhibited by 1 mM of the antioxidant N-acetyl-cystein (Figures 2e and f). Knockdown of Cx36 increased IL-1β + IFN-γ-induced ROS–RNS production (Figure 2e), whereas the overexpression of Cx36 prevented it (Figure 2f). As a positive control for ROS–RNS and superoxide production, INS-1E cells were treated for 30 min with 200 μM of the ROS inducer pyocyanin, which induced a 3–5 fold increase in ROS–RNS production.

Cx36 modulates the mitochondrial pathway of apoptosis.
Release of mitochondrial cytochrome c into the cytoplasm is a known feature of the mitochondrial pathway of apoptosis.[14] We assessed cytochrome c distribution by immunofluorescence in INS-1E cells treated with IL-1β + IFN-γ for 15 h and observed four distinct patterns (Figure 3a). Live (L) cells featured the typical mitochondrial network staining, whereas apoptotic cells, identified by nucleus morphology using DNA staining by Hoechst, displayed either a diffuse cytosolic cytochrome c staining (A), a discrete pattern typical of fragmented mitochondria that still retain cytochrome c (B), or occasionally no cytochrome c staining (C) (Figure 3a, left panel). Quantitative analysis revealed that about 60% of the apoptotic cells featured cytosolic cytochrome c and this fraction was significantly reduced in cells overexpressing Cx36 (Figure 3a, right panel). Western blots of Bcl-2 and Mcl-1 confirmed that the levels of these proteins were significantly decreased after a 15-h treatment with IL-1β + IFN-γ (Figures 3b and c). Cx36 knockdown using siCx36#2, which was the most efficient siRNA (Figures 2 and 3), significantly decreased basal Mcl-1 and Bcl-2 levels and tended to aggravate the cytokine-induced Mcl-1 and Bcl-2 decrease (Figure 3b). In contrast, Cx36 overexpression restored Bcl-2 levels and increased Mcl-1 levels in cells treated with IL-1β + IFN-γ (Figure 3c).

Cx36 overexpression increases ER Ca^{2+} store and prevents ER Ca^{2+} store depletion upon cytokine treatment. We previously showed that cytokines induce a
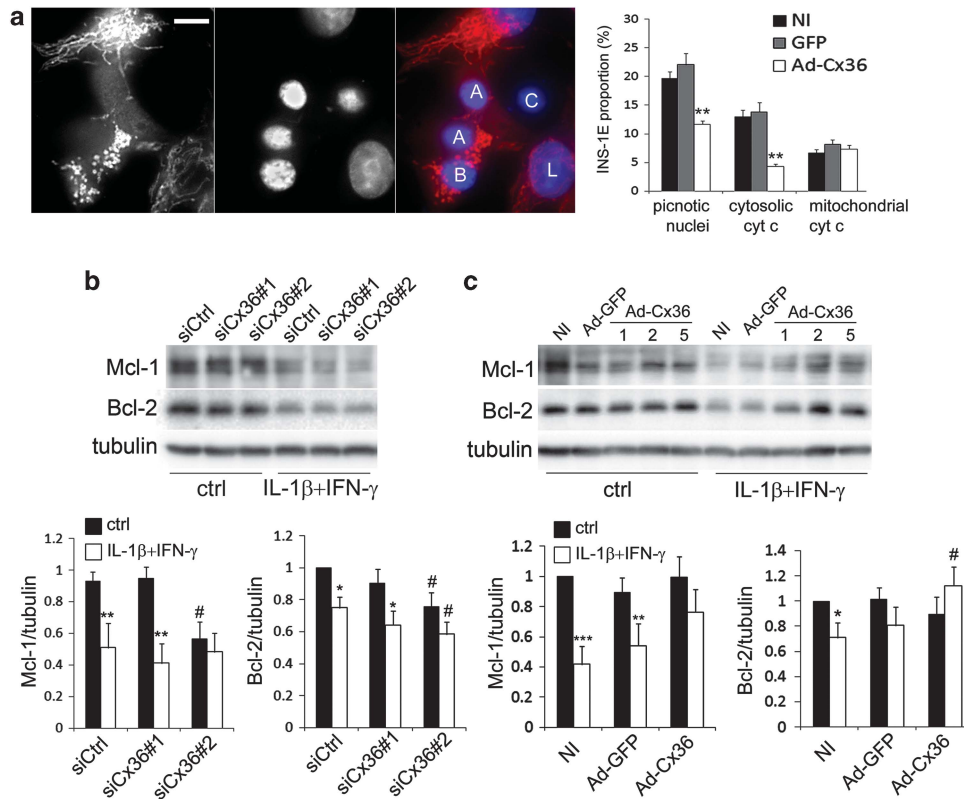
Figure 3 Changes in Cx36 expression modulate the mitochondrial pathway of apoptosis in INS-1E cells. (**a**) INS-1E cells were infected or not (NI) with Ad-Cx36 at MOI 2. Representative cytochrome c immunostaining (red) and DAPI (blue nuclear staining) upon IL-1β + IFN-γ-induced apoptosis (left panel) and quantitative assessment of picnotic nuclei and cytosolic or mitochondrial cytochrome c staining pattern (right panel). White bar: 5 μm. L: live cell; A: apoptotic cell with cytochrome c release; B: apoptotic cell without cytochrome c release; C: apoptotic cell without cytochrome c. (**b**) INS-1E cells were transfected with a control siRNA (siCtrl) or two different Cx36 siRNA (siCx36#1 and #2) and treated for 15 h with IL-1β + IFN-γ. Representative western blot for Bcl-2 and Mcl-1 over tubulin and quantitative assessment (means ± S.E.M.) of Mcl-1/tubulin (left panel) and Bcl-2/tubulin (right panel) levels from five independent experiments. *$P < 0.05$, **$P < 0.01$ versus ctrl. #$P < 0.05$ versus respective siCtrl condition. (**c**) INS-1E cells were infected or not (NI) with a control virus (Ad-GFP) or a Cx36 virus (Ad-Cx36) and treated for 15 h with IL-1β + IFN-γ. Representative western blot for Bcl-2 and Mcl-1 over tubulin and quantitative assessment (means ± S.E.M.) of Mcl-1/tubulin (left panel) and Bcl-2/tubulin (right panel) levels from six independent experiments (Ad-GFP and Ad-Cx36 at MOI2). *$P < 0.05$, **$P < 0.01$, ***$P < 0.01$ versus ctrl. #$P < 0.05$ versus respective NI condition

depletion of the ER Ca^{2+} stores,[15] leading to ER stress and β-cell apoptosis.[12,16] In an attempt to measure ER Ca^{2+}, INS-1E cells loaded with the cytosolic Ca^{2+} indicator Fura-2 were maintained in KRBH medium without Ca^{2+} and treated with 5 μM thapsigargin to induce the leaking of the cation out of the ER.[15] This resulted in a rapid rise of cytosolic [Ca^{2+}]$_i$, which depends on the Ca^{2+} concentration in this organelle (Figure 4a).[15] This first phase was followed by a second 'descending' phase where [Ca^{2+}]$_i$ returned to the basal level, which directly reflects the Ca^{2+} buffering/export capacities of the cells.[17,18] INS-1E cells treated for 15 h with IL-1β + IFN-γ displayed a reduced thapsigargin-induced [Ca^{2+}]$_i$ increase (Figure 4a), indicating that cytokines depleted the ER Ca^{2+} stores as previously shown.[15] Of note, Ca^{2+} buffering/export was slower in cytokine-treated cells, suggesting that cytokines also affected the cytosolic buffering capacity of the cells. Cx36 overexpression significantly increased the amplitude of the thapsigargin-induced release of Ca^{2+} from the ER and prevented the overall release of ER Ca^{2+} in cytokine-treated cells (Figure 4a). However, Cx36 overexpression did not have an impact on the slope of the second 'descending' phase of the curve, suggesting that Cx36 overexpression did not alter the

kinetics of Ca^{2+} buffering/export, in control or in cytokine-treated conditions (Figure 4a).

Interestingly, Cx36 knockdown sensitized, whereas Cx36 overexpression protected INS-1E cells against apoptosis induced by a 15-h treatment with the chemical ER stressors thapsigargin (100 nM) or tunicamycin (5 μg/ml) or the Ca^{2+} ionophore A23187 (1 μM) (Supplementary Figures S3a and b). Western blot analyses of the ER-stress marker CHOP revealed that Cx36 knockdown aggravated the cytokine-induced CHOP overexpression (Figure 4b and Supplementary Figure S3c), whereas Cx36 overexpression reduced it (Figure 4c and Supplementary Figure S3d). Similar effects were observed on thapsigargin-induced CHOP overexpression (Figures 4d and e). Of note, the amounts of cleaved caspase 3 closely correlated with those of CHOP in all experiments (Figures 4b–e and Supplementary Figures S3e and f). Altogether, these data indicate that Cx36 modulates in parallel ER Ca^{2+} levels, ER stress and apoptosis of INS-1E cells.

Cx36 expression is regulated by ER stress and AMPK.
IL-1β + IFN-γ stimulated the phosphorylation of AMPK (Figure 5a and Supplementary Figure S4a) in INS-1E cells and simultaneously downregulated Cx36 (Figure 5a).
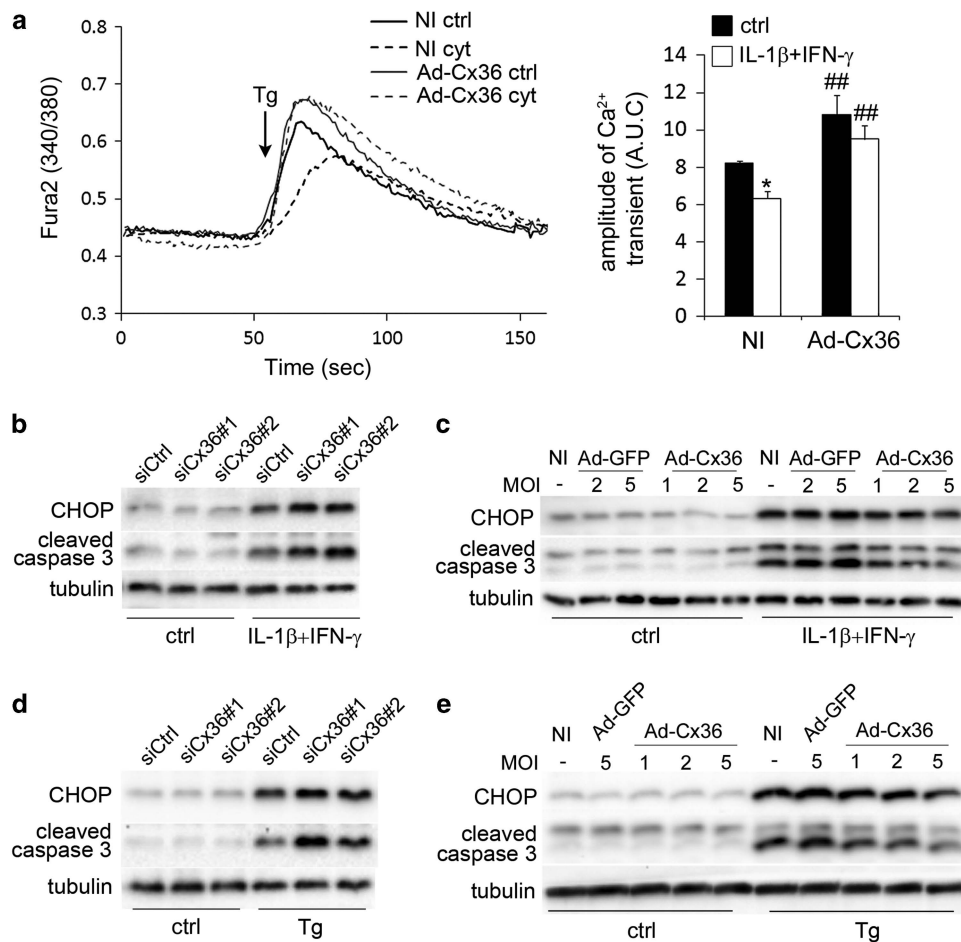
Figure 4 Changes in Cx36 expression modulate ER stress, CHOP and activate caspase 3 levels in INS-1E cells. (**a**) INS-1E cells were infected or not (NI) with a control adenovirus (Ad-GFP) or a rat Cx36 adenovirus (Ad-Cx36) at various multiplicity of infection (MOI), as indicated. Cells were then treated or not (ctrl) for 15 h with IL-1β + IFN-γ (cyt), loaded with the cytosolic calcium-dye Fura-2 and monitored in Ca^{2+}-free KRBH in presence of the SERCA inhibitor thapsigargin (Tg; 5 μM, arrow). Left panel: data are representative traces. Right panel: quantitative assessment of the cytosolic Ca^{2+} rise calculated by the area under the curve (A.U.C.) of four independent experiments. *$P < 0.05$ versus ctrl condition; ##$P <$ versus respective NI condition. (**b–d**) Representative western blot for CHOP and cleaved caspase 3 over tubulin levels in INS-1E cells transfected with a control siRNA (siCtrl) or two different Cx36 siRNA (siCx36#1 and #2) and treated for 24 h with IL-1β + IFN-γ (**b**) or for 15 h with thapsigargin (Tg: 100 nM; (**d**)). (**c–e**) Representative western blot for CHOP and cleaved caspase 3 over tubulin levels in INS-1E cells infected or not (NI) with a control adenovirus (Ad-GFP) or a rat Cx36 adenovirus (Ad-Cx36) at various MOI and treated for 24 h with IL-1β + IFN-γ (**c**) or for 15 h with thapsigargin (Tg: 100 nM; (**e**))

Co-treatment with 20 μM of the AMPK inhibitor compound C abolished the effect of IL-1β or IL-1β + IFN-γ on both AMPK phosphorylation and Cx36 downregulation (Figure 5b). Metformin and AICAR, two compounds known to activate AMPK, also decreased Cx36 expression in INS-1E cells (Supplementary Figure S4b) and compound C blocked all these effects (Supplementary Figures S4c and d). In agreement with these data, metformin reduced the coupling between INS1-E cells (Table 1). AMPK inhibition using an adenovirus allowing the overexpression of a dominant-negative form of the kinase (Ad-DN-AMPK) also prevented the effect of both metformin and IL-1β + IFN-γ on the levels of Cx36 mRNA (Supplementary Figure S4e) and protein (Figure 5c). As a positive control, we observed that the known AMPK target gene Liver-type pyruvate kinase (L-PK) was regulated like Cx36 after both AMPK activation and inhibition (Supplementary Figure S4e).

We then studied the mechanisms of cytokine-induced AMPK activation. Figure 5d shows that the cytokine-induced AMPK phosphorylation and Cx36 downregulation were both inhibited by 1 mM L-NAME (Figure 5d), suggesting an involvement of NO. In line with these data, 100 μM sodium nitroprusside (SNP) mimicked the effect of cytokines on Cx36 levels and, to a limited extent, on AMPK phosphorylation (Figure 5d). Cytokines were able to phosphorylate AMPK and decrease Cx36 despite the presence of 50 μM the pan-caspase inhibitor Z-VAD-FMK (Figure 5d), indicating that NO production and the regulation of AMPK and Cx36 are independent and precede apoptosis. Time-course analyses revealed that thapsigargin (100 nM), but not tunicamycin (data not shown), controlled Cx36, CHOP expression and AMPK phosphorylation within a same time-window (Figure 5e). The Ca^{2+} ionophore A23197 (1 μM) mimicked the effects of thapsigargin on the
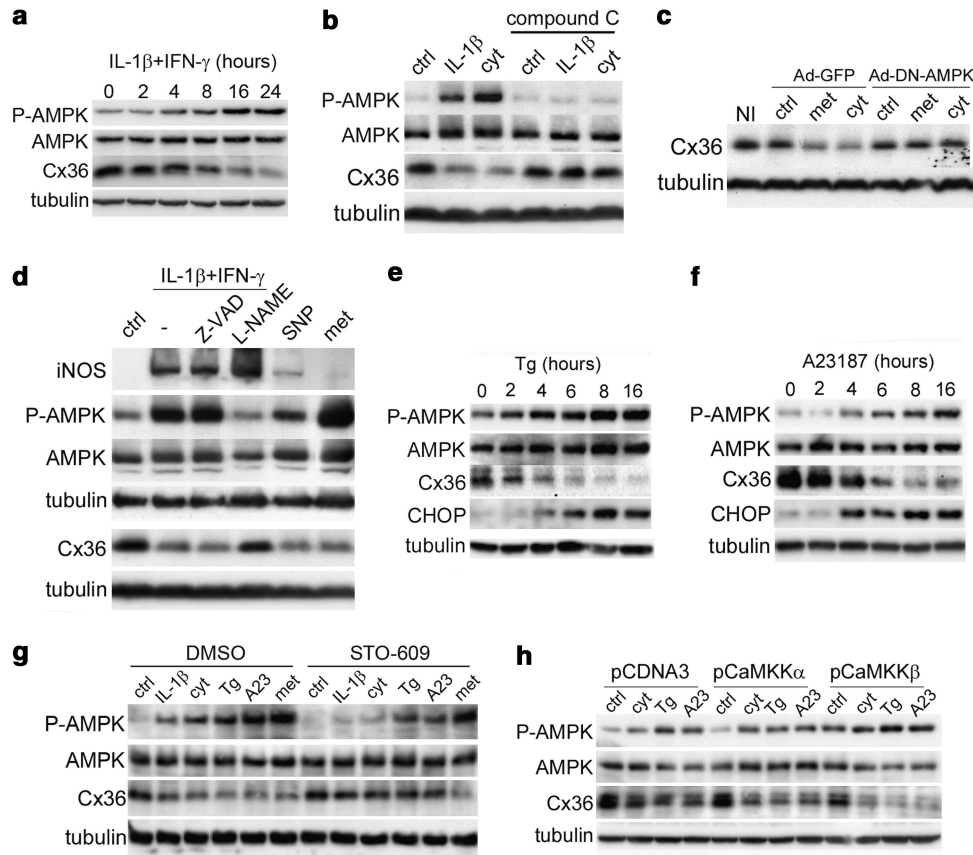
Figure 5 Cytokine-induced Cx36 downregulation requires AMPK activation in INS-1E cells. (a) Time-course analyses of P-AMPK, AMPK, Cx36 and tubulin levels in INS-1E cells treated with IL-1β + IFNγ. (b) Western blot of P-AMPK, AMPK, Cx36 and tubulin levels in INS-1E cells cultured for 24 h in the presence or absence (ctrl) of IL-1β or IL-1β + IFNγ (cyt), alone or in combination with the AMPK inhibitor compound C (20 μM). (c) INS-1E cells were infected with a control Ad-GFP virus or a dominant-negative AMPK virus (Ad-DN-AMPK) and cultured for 24 h in the absence (ctrl) or presence of metformin (met; 1 mM) or IL-1β + IFNγ (cyt). (d) Representative western blot of iNOS, P-AMPK, AMPK, Cx36 and tubulin in INS-1E cells treated for 24 h with IL-1β + IFN-γ (cyt), alone or in combination with 1 mM L-NAME or 50 μM Z-VAD, or 100 μM SNP or 1 mM metformin (met). (e and f) Time-course or dose-response analyses of P-AMPK, AMPK, Cx36 and CHOP reveal that thapsigargin and A23187 stimulated AMPK phosphorylation and Cx36 reduction in INS-1E cells. (g) Representative western blot of P-AMPK, AMPK, Cx36 and tubulin levels in INS-1E cells treated with IL-1β, IL-1β + IFN-γ (cyt), thapsigargin (Tg), A23187 (A23) or metformin (met) for 16 h, together with DMSO or the CaMKKs inhibitor STO-609. (h) Representative western blot of P-AMPK, AMPK, Cx36 and tubulin in INS-1E cells transfected with an empty vector (ctrl) or vectors encoding either CaMKKα or CaMKKβ, and treated for 15 h with IL-1β + IFN-γ (cyt), thapsigargin (Tg) or A23187 (A23)
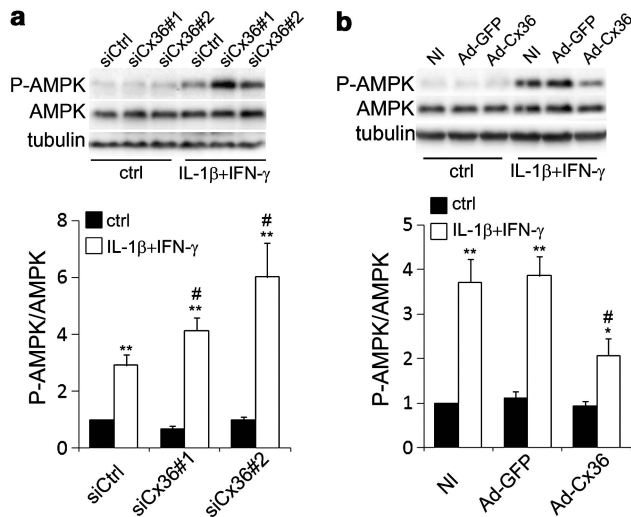
expression of Cx36 and CHOP and on the phosphorylation of AMPK (Figure 5f), suggesting that cytosolic Ca^{2+} as a plausible link between the different conditions that control Cx36 expression.

AMPK phosphorylation/activation is controlled by several kinases.[19] The Ca^{2+}-activated Ca^{2+}/calmodulin-dependent kinase kinases (CaMKKs) inhibitor STO-609[20] partly blocked the effects of IL-1β + IFN-γ, thapsigargin (100 nM) and A23187 (1 μM), but not metformin (1 mM), on AMPK phosphorylation and Cx36 levels (Figure 5g). In addition, transient overexpression of a constitutively active form of CaMKKβ, but not CaMKKα (Supplementary Figure S5a), increased the basal levels of P-AMPK and potentiated the effects of IL-1β + IFN-γ, thapsigargin and A23187 on these levels (Figure 5h and Supplementary Figure S5b), enhancing the downregulation of Cx36 (Figure 5h and Supplementary Figure S5c). In contrast, LKB1 knockdown using two siRNAs (Supplementary Figure S6a) did not affect the downregulation of Cx36 induced by IL-1β + IFN-γ,

thapsigargin or A23187 (Supplementary Figures S6b–d), whereas it partially blocked the effects of IL-1β + IFN-γ, thapsigargin and A23187 on AMPK phosphorylation (Supplementary Figures S6b and c). Collectively, these experiments suggest that both LKB1 and CaMKKβ are involved in the cytokine-induced AMPK phosphorylation and that only CaMKKβ-mediated AMPK phosphorylation selectively leads to Cx36 downregulation.

Cytokine-induced Cx36 downregulation triggers a positive feedback loop of AMPK activation. Cx36 downregulation aggravates ER stress (Figure 3), and cytokine-induced ER stress stimulates AMPK phosphorylation, leading to Cx36 downregulation (Figure 5). We tested the effect of Cx36 knockdown or overexpression on cytokine-induced AMPK phosphorylation. Cx36 knockdown increased cytokine-induced P-AMPK levels, whereas Cx36 overexpression slightly decreased the P-AMPK levels (Figures 6a and b).

Cytokines inhibit Cx36 transcription via a cAMP response element in the *GJD2* promoter. The stability of the Cx36 transcript was not altered by a 15-h exposure to either 1 mM metformin or 50 U/ml IL-1β, as indicated by the time-course treatments with 5 μg/ml actinomycin D,

suggesting that the AMPK-dependent control of Cx36 occurs at the transcriptional level (Figure 7a).

To identify the region of the Cx36 gene responsible for the AMPK effect, INS-1E cells were transiently transfected with four fragments of the promoter of the human Cx36 gene *GJD2* and then exposed for 24 h to either 1 mM metformin, 50 U/ml IL-1β or 10 U/ml IL-1β + 100 U/ml IFN-γ. All constructs, but the pGL3-316, displayed a 20–30% reduction in the response to both metformin and cytokines. Mutation of a cAMP response element (CRE) involved in the transcriptional activity of *GJD2*[21,22] restored the activity of the *GJD2* promoter in response to all treatments (Figure 7b). AMPK hampers CRE activities by inhibiting the nuclear translocation of the Crtc2.[23,24] Transient overexpression of mouse Crtc2 (Figure 7c) stimulated the activity of the wild type *GJD2* promoter but not that of the promoter containing the CRE-mutated fragment (Figure 7d). Furthermore, Crtc2 over-expression restored the Cx36 transcript levels to the control value in INS-1E cells treated with IL-1β + IFN-γ (Figure 7e).

Figure 6 Changes in Cx36 expression modulate ER stress-induced phosphorylation of AMPK in INS-1E cells. (**a**) Representative western blot and quantification of P-AMPK over AMPK levels in INS-1E cells transfected with a control siRNA (siCtrl) or two different Cx36 siRNAs (siCx36#1 and #2) and treated for 24 h with IL-1β + IFN-γ. (**b**) Representative western blot and quantification of P-AMPK over AMPK levels in INS-1E cells infected or not (NI) with the Ad-GFP or the Ad-Cx36 at various multiplicity of infection (MOI), as indicated, and treated for 24 h with IL-1β + IFN-γ. *$P<0.05$, **$P<0.01$ *versus* ctrl. #$P<0.05$ *versus* respective siCtrl condition or NI condition

Discussion

We have previously shown that loss of the native gap junction protein Cx36 sensitizes pancreatic β-cells to death in mice models of hyperglycemia induced *in vivo* by the administration of either alloxan or streptozotocin, and that, conversely, the experimental overexpression of Cx36 protects against these insults.[4] Cx36 also protects pancreatic β-cells *in vitro* against apoptosis induced by lipids[22,25] and cytokines.[4] Although these studies suggest a common pathway for Cx36-mediated protection against various cytotoxic insults both *in vitro* and *in vivo,* the molecular mechanisms activating this pathway remain to be unraveled. The aim of this study was to identify
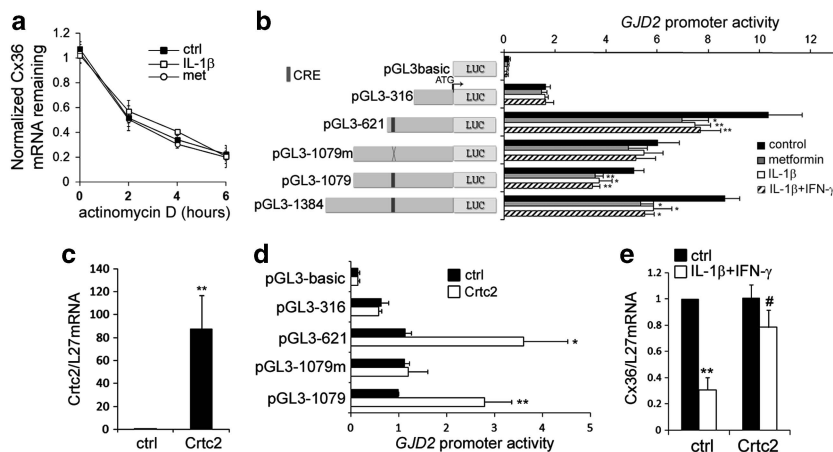
Figure 7 Crtc2 is involved in cytokine-induced inhibition of Cx36 transcriptional activity. (**a**) INS-1E cells were incubated for 2, 4 or 6 h in the absence (ctrl; black squares) or presence of IL-1β (white squares) or metformin (white circles), together or not (t0) with the transcription inhibitor actinomycin D. Data are means ± S.E.M. of Cx36/L27 mRNA levels assessed by qPCR in three independent experiments. (**b**) INS-1E cells were cotransfected with a plasmid expressing the reporter gene luciferase under the control of progressive deletions of the human *GJD2* promoter, including one construct with a mutated CRE (pGL3-1079m). After transfection, cells were incubated for 24 h in absence (control; black bars) or presence of metformin (gray bars), IL-1β (white bars) or IL-1β + IFN-γ (striped bars). Data are mean ± S.E.M. of 4–7 independent experiments. *$P<0.05$; **$P<0.01$ *versus* ctrl. (**c**) Quantitative RT-PCR analyses of Crtc2 over L27 mRNA levels in INS-1E cells transfected with a Crtc2-coding plasmid or a control empty vector (ctrl). Data are mean ± S.E.M. of four independent experiments. **$P<0.01$ *versus* respective empty vector transfection. (**d**) Luciferase activity in INS-1E cells cotransfected with various *GJD2* promoter constructs and a control empty vector (ctrl; black bars) or the Crtc2-coding plasmid (Crtc2; white bars). Data are mean ± S.E.M. of five independent experiments. *$P<0.05$; **$P<0.01$ *versus* empty vector transfection. (**e**) Quantitative RT-PCR analyses of Cx36 over L27 mRNA levels in INS-1E cells transfected with a control plasmid (ctrl) or the Crtc2-coding plasmid (Crtc2) and treated or not (black bars) for 24 h with IL-1β + IFN-γ (white bars). Data are mean ± S.E.M. of four independent experiments. **$P<0.01$ *versus* untreated cells. #$P<0.05$ *versus* respective empty vector transfection
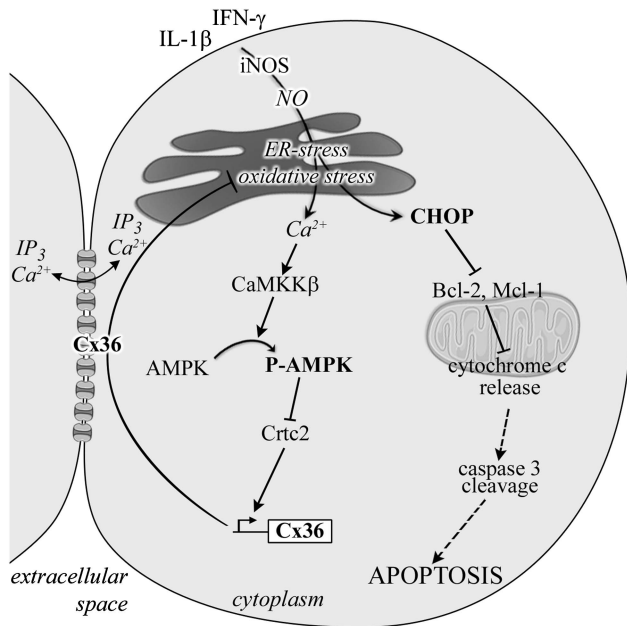
Figure 8 Cx36 has a central role in cytokine-induced ER stress, AMPK regulation and apoptosis. Pro-inflammatory cytokines stimulate NO production, leading to ER stress and increased CHOP expression. The ER stress-mediated $[Ca^{2+}]_I$ increase promotes CaMKKβ activation, resulting in AMPK phosphorylation, inhibition of Crtc2 and the subsequent Cx36 downregulation. The decline in Cx36 levels aggravates ER stress, leading to increased CHOP overexpression, which in turn facilitates the degradation of the anti-apoptotic proteins Bcl-2 and Mcl-1, leading to cytochrome c release and, eventually, apoptosis. In a feedback loop, the reduced Cx36 levels facilitate AMPK phosphorylation, which further contributes to decrease in the levels of Cx36 and to worsening of the ER stress

these mechanisms, specifically those contributing to the β-cell apoptosis induced by the pro-inflammatory cytokines involved in the pathophysiology of type 1 diabetes.[5] Here, we first demonstrate that cytokines and chemical ER stressors decrease the expression of Cx36 by downregulating the transcription of the cognate *GJD2* gene. This effect requires the Ca^{2+}-mediated activation of AMPK by CaMKKβ, and the subsequent inhibition of Crtc2, a CREB cofactor that modulates the activity of the *GJD2* promoter. By altering the expression of Cx36 using siRNA and adenoviral gene transfer strategies, we then document that the knockdown of Cx36 sensitizes insulin-producing cells to the apoptosis induced by pro-inflammatory cytokines (IL-1β, TNF-α and IFN-γ), whereas the overexpression of Cx36 protects against this effect. We further document that these effects correlate with oxidative stress. Thus, the knockdown of Cx36 increases the cytokine-induced production of both ROS and NO, whereas the overexpression of Cx36 prevents against this effect. Although more studies are required to carefully assess the impact of Cx36 on ER Ca^{2+} levels, the study of ER Ca^{2+} release in the cytosol also suggest that Cx36 overexpression increases the basal ER Ca^{2+} levels. As a result, Cx36 overexpression dampens the depleting effect of cytokines on INS-1E cells and subsequent stress at the level of the ER. Accordingly, Cx36 overexpression lessens the effects of cytokines on ER stress-induced overexpression of CHOP, degradation of anti-apoptotic proteins Mcl-1 and Bcl-2,

release of intra-mitochondrial cytochrome c, caspase 3 cleavage and, ultimately, apoptosis. Together, the activation of the mitochondria-dependent apoptosis and the concurrent downregulation of Cx36 following ER stress and the subsequent AMPK activation may contribute to the impairment of the β-cell resistance to cytokines (Figure 8).

Cytokines trigger ER stress in β-cells in an NO-dependent manner, through the downregulation of Serca2 and the subsequent depletion of ER Ca^{2+} stores.[15] Cytokines are also known to stimulate AMPK activity in β-cells,[26] but the mechanisms underlying this activation remained unclear. Here we show that AMPK activation requires the production of NO, and can be achieved with thapsigargin but not with tunicamycin, suggesting that the depletion of ER Ca^{2+} and the subsequent increase in cytosolic Ca^{2+} concentration, rather than the ER stress *per se*, trigger the activation of the kinase. The activation of the AMPK complex is controlled by several upstream kinases,[13] including the constitutively active kinase LKB1[19,27–29] and the Ca^{2+}-activated CaMKKs.[19,30,31] Our data demonstrate that cytokines and thapsigargin phosphorylate AMPK via both LKB1 and CaMMKβ, but that only the latter kinase controls the expression of Cx36 in INS-1E cells. This discrepancy between AMPK and Cx36 regulation may be due to the fact that β-cells express both AMPKα1 and AMPKα2,[32] two isoforms with partly redundant actions, but different localizations[32] and preferential targets.[33–35] The negative effect of AMPK on Cx36 transcriptional activity is mediated by inhibition of Crtc2, and it could be that only a CaMKKβ-activated pool of AMPK is inhibiting Crtc2 and Cx36 expression.

We have previously shown that diabetogenic conditions such as high glucose, palmitate and/or oxidized LDL particles downregulate the expression of the Cx36 gene *GJD2* through a cAMP/PKA-dependent overexpression of the repressor ICER-1/ICER-1γ.[21,36] The present study unveils a novel pathway whereby cytokines downregulate Cx36 expression through a Ca^{2+}- and CaMMKβ-dependent activation of AMPK. We further document that the levels of AMPK, Cx36 and cell apoptosis are tightly related. Our data extend the notion that a persistent activation of AMPK leads to β-cell apoptosis, which has been suggested to involve the c-jun N-terminal kinase[37,38] as well as the anti-apoptotic mTOR pathways.[39] We propose that Cx36 downregulation is an additional pro-apoptotic mechanism explaining the deleterious impact of sustained AMPK activation on β-cell survival. Strikingly, the downregulation of Cx36 triggers a feedback loop, whereby the decreased connexin expression enhances the cytokine-induced ER stress, the activation of AMPK and the overexpression of CHOP, leading to further Cx36 downregulation and, eventually, apoptosis (Figure 8).

The sequence of events induced by cytokines leading to β-cell apoptosis is still incompletely understood. Here, we observe that Cx36 overexpression decreases the cytokine-induced production of ROS, but that neither the knockdown nor the overexpression of Cx36 influences the basal and the cytokine-induced production of NO (data not shown).[4] This indicates that the effect of Cx36 on ROS–RNS production occurs downstream the generation of NO. Furthermore, since Cx36 overexpression protects INS-1E cells against the thapsigargin-induced apoptosis, the cytokine-induced ROS

production is likely to be secondary to the release of ER Ca^{2+} and to the ensuing ER stress. Our data suggest that the cytosolic concentration of free Ca^{2+} has a central role in the cross talk between ER stress, AMPK activity and Cx36 signaling and regulation. This is consistent with previous studies showing a critical role of the cation in the activation of ER stress, the generation of ROS, the control of mitochondrial function[40] and the activation of AMPK.[41] Cx36 overexpression increases the basal Ca^{2+} stores of ER and prevents their depletion after exposure to cytokines (present data), whereas loss of Cx36 impairs the intercellular synchronization of Ca^{2+} transients,[42–45] whose generation requires proper ER Ca^{2+} stores.[46] The homeostasis of ER Ca^{2+} is controlled by many factors, including inositol 1,4,5-trisphosphate (IP3), which can permeate gap junctions and contribute to mitochondrial apoptosis.[47] Therefore, it is plausible that, by allowing the intercellular diffusion of Ca^{2+} and/or IP3, Cx36 channels achieve a sufficient dilution of harmful signals across the population of coupled cells, thus preventing the activation of mitochondrial apoptosis.[4] Consistent with this hypothesis, Cx36 specifically hampers the intrinsic mitochondrial pathway of apoptosis by modulating the effect of cytokines on the Ca^{2+} stores of the ER and on the expression of the CHOP, Bcl-2 and Mcl-1 proteins. These data further confirm our previous findings that CHOP has an important role in cytokine-induced apoptosis of insulin-producing cells by altering the stability of the Bcl-2 and Mcl-1 proteins.[12]

Overall, our data document that, by preserving the ER Ca^{2+} stores, Cx36-mediated intercellular communication prevents the cytokine-mediated ER stress, the subsequent activation of AMPK and the mitochondria-dependent apoptosis of INS-1E cells (Figure 8). Altogether, our data underscore the novel, central roles of AMPK and Cx36 in the pro-apoptotic events leading to β-cell apoptosis. In this scenario, innovative therapeutic approaches to interfere with the β-cell destruction in the context of T1D should benefit of the association of drugs restricting AMPK activation and of drugs promoting the expression and function of Cx36. The availability of novel methods for the screening of such specifically targeted drugs[43,48] will be instrumental to test this exciting possibility.

Materials and Methods

Materials. The following chemicals were purchased from Sigma-Aldrich NV/SA (Bornem, Belgium) and used as indicated: A23187 (1 μM), thapsigargin (100 nM or 5 μM), tunicamycin (5 μg/ml) and STO-609 (10 μM) were dissolved in DMSO; NG-Methyl-L-arginine (L-NMMA, 1 mM), sodium nitroprusside (SNP; 100 μM) and N-acetyl-cystein (NAC; 1 mM) were dissolved in distilled water. The following cytokines were used: recombinant human IL-1β (R&D systems, Abingdon, UK) at 10 U/ml in experiments with INS-1E cells; recombinant rat IFN-γ (R&D systems) at 100 U/ml (7.2 ng/ml) in experiments with INS-1E cells;[15,16] recombinant human TNF-α (R&D systems) at 1000 U/ml in all experiments. The concentrations of chemicals and cytokines were selected based on our previous dose-response studies.[15]

Cells and islets. The rat insulinoma cell line INS-1E (kindly provided by Professor Pierre Maechler, CMU, University of Geneva) was maintained in complete RPMI 1640 medium, as previously described.[16,21] C57Bl6/J mice and male Wistar rats (Janvier, St Berthevin, France) islets were isolated by collagenase digestion followed by hand picking under a stereomicroscope.[16,21] Mouse and rat care, surgery and euthanasia procedures were approved by the Centre Hospitalier Universitaire Vaudois (CHUV) and the Cantonal Veterinary Office (Service de la Consommation et des Affaires Vétérinaires SCAV-EXPANIM).

RNA isolation and quantitative RT-PCR. Cells were homogenized in Tripure Isolation Reagent (Roche Diagnostics AG, Rotkreuz, Switzerland) and total RNA was extracted using the kit procedure. Transcripts (1 μg) were reverse-transcribed using ImProm-II Reverse transcription System (Catalys AG, Wallisellen, Switzerland). Quantitative PCR was performed in a StepOne plus apparatus, using the Applied Biosystems Fast SYBR Green Master mix (Life Technologies Europe B.V., Zug, Switzerland). The primers used for amplification are given in Supplementary Table S1. Expression values were normalized to the ribosomal protein L27 (Rpl27).

Immunofluorescence. INS-1E cells grown on glass coverslips were fixed for 5 min in $-20\,^{\circ}$C acetone, air-dried, rinsed in PBS and permeabilized for 1 h in PBS supplemented with 1.5% BSA and 0.1% Triton X-100 (full PBS). Cytochrome c was immunostained on INS-1E cells fixed for 5 min in 4% ice-cold PFA, rinsed in PBS and permeabilized for 1 h in full PBS. In both cases, the coverslips were incubated overnight at 4 $^{\circ}$C in the presence of either a rabbit polyclonal serum against Cx36 (dilution 1/100; Invitrogen) or a mouse monoclonal against cytochrome c (1/1000; BD Biosciences, Allschwil, Swizterland). Cells were then washed and further exposed for 1 h to an appropriate Alexa fluor 488- or 555-conjugated antibody (1/1000; Life Technologies Europe B.V.) and photographed under fluorescence microscopy (Leica Camera AG, Nidau, Switzerland). Quantitative assessment of the membrane spots immunostained by the Cx36 antibodies was performed using the ImageJ software. Briefly, 30 images from 3 distincts experiments were first converted to a 32-bit format and the signal-to-noise ratio was determined by applying the Yen thresholding method.[49] A binary image was then created and the pixel intensity of the Cx36 signal was calculated. Data were normalized to the number of cells in each image.

Transient transfection and promoter reporter assays. INS-1E cells were transiently transfected using lipofectamine 2000 (Life Technologies Europe B.V.) as previously described.[22,36] The CaMKKα and β CDS plasmids cloned in pCDNA3 were kindly provided by Dr Angela Woods (MRC Clinical Science Centre, Imperial College, Hammersmith Hospital, London, England). The mouse Crtc2 CDS plasmid was purchased from Origene (OriGene Technologies, Rockville, MD, USA). Promoter studies were performed using various fragments of the promoter of the human Cx36 gene *GJD2*, which was cloned in the pGL3-basic reporter plasmid, as previously described.[36] The Luciferase plasmids were cotransfected with the internal control pRL-CMV encoding

Renilla luciferase (Promega, Madison, WI, USA). The transcriptional activity of *GJD2* was assessed using the Dual-Luciferase reporter assay system (Catalys AG) in a Turner TD-20/20 Luminometer.[21] The activity of the *GJD2* promoter was normalized to that induced by the pRL-CMV plasmid, which was cotransfected.

Western blot analysis. Cells were washed once with cold PBS and immediately lysed in Laemmli buffer as previously described.[16,21] Lysates were resolved by SDS-PAGE and transferred to a PVDF membrane. Immunoblot analyses were performed as previously described,[16,21] using the following antibodies: rabbit polyclonal antibodies against Cx36 diluted 1:200;[21,36] rabbit polyclonal anti P-AMPKα1 and α2, diluted 1:1000; rabbit polyclonal anti-total AMP-Kα1,α2, diluted 1:2000; rabbit polyclonal anti-LKB1, diluted 1:1000; polyclonal anti-cleaved caspase 3, diluted 1:1000 from Cell Signaling Boston, MA, USA; polyclonal anti-Bcl-2, diluted 1:1000; polyclonal anti-CHOP/GADD153, diluted 1:1000 and polyclonal anti-Bax, diluted 1:1000; from Santa Cruz Biotechnology, Santa Cruz, CA, USA; rabbit anti-rat Mcl-1 (Biovision, LuBioScience GmbH, Lucerne, Switzerland) diluted 1:500; monoclonal anti-α-tubulin and horse-radish peroxidase-conjugated goat anti-rabbit or anti-mouse IgG (Sigma-Aldrich), diluted 1:5000.

RNA interference and adenoviral cell infection. Rat Cx36 *Silencer* Select pre-designed siRNA s132237 (siCx36#1) and s132238 (siCx36#2) and rat LKB1 *Silencer* Select pre-designed siRNA s163339 (siLKB1#1) and s163340 (siLKB1#2) were from Applied Biosystems (Life Technologies Europe B.V.). The Allstars Negative Control siRNA (Qiagen, Hombrechtikon, Switzerland), which has no effect on β-cell gene expression and viability,[12,16,50] was used as a control. siRNA transfections were conducted as previously described using lipofectamin RNAiMax (Life Technologies Europe B.V.) and 30 nM siRNA. The efficiency of transfection was >90% of the cells.[12,16,50] The Control Ad-GFP and Ad-Cx36 viruses were generated as previously described.[21,22] Ad-DN-AMPK was a kind gift from Professor Bernard Thorens, University of Lausanne, Switzerland.[51] All viral vectors were amplified and purified by Vector Biolabs, Philadelphia, PA, USA. Adenoviral infections were conducted as previously described.[16,22,52]

ROS and/or RNS and superoxide measurements. The ROS–RNS and superoxide production were measured using the total ROS and Superoxide Detection Kit (Enzo Life Sciences AG, Lausen, Switzerland) as previously described.[25] Briefly, INS-1E cells were plated in 96-well plates. Cells were transfected or infected as previously described and then treated for 24 h with IL-1β + IFN-γ. As a positive control, INS-1E cells were treated for 30 min with 200 μM of the ROS inducer pyocyanin. INS-1E cells were then washed once and incubated for 30 min in 100 μl buffer containing 2 μM oxidative stress detection reagent (green) and 2 μM superoxide detection reagent (orange). Fluorescence was quantified using the Synergy Mx Monochromator-Based Multi-Mode Microplate Reader (BioTek AG, Luzern, Switzerland) and fluorescein (Ex = 488 nm, Em = 520 nm) and rhodamine (Ex = 550 nm, Em = 610 nm) filter sets.

Cytosolic calcium monitoring. Cells were washed once in KRBH (20 mM NaCl, 3.5 mM KCl, 0.5 mM NaH_2PO_4, 1.5 mM $CaCl_2$, 5 mM $NaHCO_3$, 10 mM HEPES and 5 mM glucose) and incubated for 30 min in the same solution supplemented with 3 μM Fura-2/AM (Life Technologies Europe B.V.), in the dark and at 37 °C. Loaded cells were washed in Ca^{2+}-free KRBH containing 0.1 mM EGTA and observed under a Zeiss inverted microscope (x40 oil immersion fluorescence objective). Fura-2AM was excited at 340/380 nm with a Visichrome holographic monochromator (Visitron Systems GmbH, Puchheim, Germany) and emission fluorescence was monitored at 510 nm using a Hamamatsu Orca ER coded CCD Camera (Hamamatsu, Solothurn, Switzerland). Images were treated with MetaFluor (Molecular Devices France, St. Grégoire, France) to evaluate the ratio of fluorescence emitted at 340 and 380 nm.

Assessment of cell viability. The percentage of viable, apoptotic and necrotic cells was determined using the DNA-binding dyes propidium iodide (PI, 5 μg/ml) and Hoechst 33342 (HO, 5 μg/ml, Sigma-Aldrich).[15] The cells were examined by inverted fluorescence microscopy (Axiovert 200, Carl Zeiss, Zaventem, Belgium). A minimum of 500 cells were counted in each experimental condition by two independent observers, one of them unaware of the sample identity.

Cell coupling. Three-day-old cultures of INS-1E cells were exposed for 24 h to RPMI 1640 medium supplemented with either 10 U/ml IL-1β or 2 mM metformin. The dishes were then transferred onto the heated (37 °C) stage of an inverted Zeiss ICM35 microscope, and individual cells were microinjected using glass pipettes containing 4% Lucifer Yellow CH (Sigma-Aldrich, St Louis, MO, USA) in 10 mM Hepes-buffered (pH 7.2) 150 mM LiCl and square negative pulses of 0.1 nA amplitude, 900 ms duration and 0.5 Hz frequency. Coupling extent was calculated after each injection by scoring the number of cells containing the injected tracer. Coupling incidence was determined by calculating the percentage of injections resulting in the cell-to-cell transfer of the tracers. Coupling index was given by coupling extent × coupling incidence.

Statistical analysis. Data are presented as mean ± S.E.M. Comparisons were performed by two-tailed paired Student's *t*-test or by one-way ANOVA followed by t-tests with Bonferroni correction for multiple comparisons. Coupling incidence was compared by the χ^2-test. A *P*-value ≤0.05 was considered statistically significant.

Conflict of Interest
The authors declare no conflict of interest.

1. Bosco D, Haefliger JA, Meda P. Connexins: key mediators of endocrine function. *Physiol Rev* 2011; **91**: 1393–1445.
2. Cigliola V, Chellakudam V, Arabieter W, Meda P. Connexins and beta-cell functions. *Diabetes Res Clin Pract* 2013; **99**: 250–259.

3. Decrock E, Vinken M, De Vuyst E, Krysko DV, D'Herde K, Vanhaecke T *et al*. Connexin-related signaling in cell death: to live or let die? *Cell Death Differ* 2009; **16**: 524–536.

4. Klee P, Allagnat F, Pontes H, Cederroth M, Charollais A, Caille D *et al*. Connexins protect mouse pancreatic beta cells against apoptosis. *J Clin Invest* 2011; **121**: 4870–4879.

5. Eizirik DL, Colli ML, Ortis F. The role of inflammation in insulitis and beta-cell loss in type 1 diabetes. *Nat Rev Endocrinol* 2009; **5**: 219–226.

6. Thomas HE, McKenzie MD, Angstetra E, Campbell PD, Kay TW. Beta cell apoptosis in diabetes. *Apoptosis* 2009; **14**: 1389–1404.

7. Robertson RP. Beta-cell deterioration during diabetes: what's in the gun? *Trends Endocrinol Metab* 2009; **20**: 388–393.

8. Gurzov EN, Eizirik DL. Bcl-2 proteins in diabetes: mitochondrial pathways of beta-cell death and dysfunction. *Trends Cell Biol* 2011; **21**: 424–431.

9. Youle RJ, Strasser A. The BCL-2 protein family: opposing activities that mediate cell death. *Nat Rev Mol Cell Biol* 2008; **9**: 47–59.

10. Rasola A, Bernardi P. Mitochondrial permeability transition in Ca(2 +)-dependent apoptosis and necrosis. *Cell Calcium* 2011; **50**: 222–233.

11. Rizzuto R, De Stefani D, Raffaello A, Mammucari C. Mitochondria as sensors and regulators of calcium signalling. *Nat Rev Mol Cell Biol* 2012; **13**: 566–578.

12. Allagnat F, Fukaya M, Nogueira TC, Delaroche D, Welsh N, Marselli L *et al*. C/EBP homologous protein contributes to cytokine-induced pro-inflammatory responses and apoptosis in beta-cells. *Cell Death Differ* 2012; **19**: 1836–1846.

13. Hardie DG, Ross FA, Hawley SA. AMPK: a nutrient and energy sensor that maintains energy homeostasis. *Nat Rev Mol Cell Biol* 2012; **13**: 251–262.

14. Scorrano L. Opening the doors to cytochrome c: changes in mitochondrial shape and apoptosis. *Int J Biochem Cell Biol* 2009; **41**: 1875–1883.

15. Cardozo AK, Ortis F, Storling J, Feng YM, Rasschaert J, Tonnesen M *et al*. Cytokines downregulate the sarcoendoplasmic reticulum pump Ca2 + ATPase 2b and deplete endoplasmic reticulum Ca2 +, leading to induction of endoplasmic reticulum stress in pancreatic beta-cells. *Diabetes* 2005; **54**: 452–461.

16. Allagnat F, Cunha D, Moore F, Vanderwinden JM, Eizirik DL, Cardozo AK. Mcl-1 downregulation by pro-inflammatory cytokines and palmitate is an early event contributing to beta-cell apoptosis. *Cell Death Differ* 2011; **18**: 328–337.

17. Lemmens R, Larsson O, Berggren PO, Islam MS. Ca2 + -induced Ca2 + release from the endoplasmic reticulum amplifies the Ca2 + signal mediated by activation of voltage-gated L-type Ca2 + channels in pancreatic beta-cells. *J Biol Chem* 2001; **276**: 9971–9977.

18. Chen L, Koh DS, Hille B. Dynamics of calcium clearance in mouse pancreatic beta-cells. *Diabetes* 2003; **52**: 1723–1731.

19. Fogarty S, Hawley SA, Green KA, Saner N, Mustard KJ, Hardie DG. Calmodulin-dependent protein kinase kinase-beta activates AMPK without forming a stable complex: synergistic effects of Ca2 + and AMP. *Biochem J* 2010; **426**: 109–118.

20. Tokumitsu H, Inuzuka H, Ishikawa Y, Ikeda M, Saji I, Kobayashi R. STO-609 a specific inhibitor of the Ca(2 +)/calmodulin-dependent protein kinase kinase. *J Biol Chem* 2002; **277**: 15813–15818.

21. Allagnat F, Alonso F, Martin D, Abderrahmani A, Waeber G, Haefliger JA. ICER-1gamma overexpression drives palmitate-mediated connexin36 down-regulation in insulin-secreting cells. *J Biol Chem* 2008; **283**: 5226–5234.

22. Haefliger JA, Martin D, Favre D, Petremand J, Mazzolai L, Abderrahmani A *et al*. Reduction of Connexin36 content by ICER-1 contributes to insulin-secreting cells apoptosis induced by oxidized LDL particles. *PLoS One* 2013; **8**: e55198.

23. Lee JM, Seo WY, Song KH, Chanda D, Kim YD, Kim DK *et al*. AMPK-dependent repression of hepatic gluconeogenesis via disruption of CREB.CRTC2 complex by orphan nuclear receptor small heterodimer partner. *J Biol Chem* 2010; **285**: 32182–32191.

24. Fu A, Screaton RA. Using kinomics to delineate signaling pathways: control of CRTC2/TORC2 by the AMPK family. *Cell Cycle* 2008; **7**: 3823–3828.

25. Haefliger JA, Martin D, Favre D, Petremand Y, Mazzolai L, Abderrahmani A *et al*. Reduction of connexin36 content by ICER-1 contributes to insulin-secreting cells apoptosis induced by oxidized LDL particles. *PLoS One* 2013; **8**: e55198.

26. Riboulet-Chavey A, Diraison F, Siew LK, Wong FS, Rutter GA. Inhibition of AMP-activated protein kinase protects pancreatic beta-cells from cytokine-mediated apoptosis and CD8 + T-cell-induced cytotoxicity. *Diabetes* 2008; **57**: 415–423.

27. Ollila S, Makela TP. The tumor suppressor kinase LKB1: lessons from mouse models. *J Mol Cell Biol* 2011; **3**: 330–340.

28. Lizcano JM, Goransson O, Toth R, Deak M, Morrice NA, Boudeau J *et al*. LKB1 is a master kinase that activates 13 kinases of the AMPK subfamily, including MARK/PAR-1. *Embo J* 2004; **23**: 833–843.

29. Hawley SA, Boudeau J, Reid JL, Mustard KJ, Udd L, Makela TP *et al*. Complexes between the LKB1 tumor suppressor, STRAD alpha/beta and MO25 alpha/beta are upstream kinases in the AMP-activated protein kinase cascade. *J Biol* 2003; **2**: 28.

30. Woods A, Dickerson K, Heath R, Hong SP, Momcilovic M, Johnstone SR *et al*. Ca2 + / calmodulin-dependent protein kinase kinase-beta acts upstream of AMP-activated protein kinase in mammalian cells. *Cell Metab* 2005; **2**: 21–33.

31. Hawley SA, Pan DA, Mustard KJ, Ross L, Bain J, Edelman AM *et al*. Calmodulin-dependent protein kinase kinase-beta is an alternative upstream kinase for AMP-activated protein kinase. *Cell Metab* 2005; **2**: 9–19.

32. da Silva Xavier G, Leclerc I, Salt IP, Doiron B, Hardie DG, Kahn A *et al*. Role of AMP-activated protein kinase in the regulation by glucose of islet beta cell gene expression. *Proc Natl Acad Sci USA* 2000; **97**: 4023–4028.

33. Woods A, Salt I, Scott J, Hardie DG, Carling D. The alpha1 and alpha2 isoforms of the AMP-activated protein kinase have similar activities in rat liver but exhibit differences in substrate specificity in vitro. *FEBS Lett* 1996; **397**: 347–351.

34. Klaus A, Polge C, Zorman S, Auchli Y, Brunisholz R, Schlattner U. A two-dimensional screen for AMPK substrates identifies tumor suppressor fumarate hydratase as a preferential AMPKalpha2 substrate. *J Proteomics* 2012; **75**: 3304–3313.

35. Witczak CA, Sharoff CG, Goodyear LJ. AMP-activated protein kinase in skeletal muscle: from structure and localization to its role as a master regulator of cellular metabolism. *Cell Mol Life Sci* 2008; **65**: 3737–3755.

36. Allagnat F, Martin D, Condorelli DF, Waeber G, Haefliger JA. Glucose represses connexin36 in insulin-secreting cells. *J Cell Sci* 2005; **118**(Pt 22): 5335–5344.

37. Kefas BA, Cai Y, Kerckhofs K, Ling Z, Martens G, Heimberg H *et al*. Metformin-induced stimulation of AMP-activated protein kinase in beta-cells impairs their glucose responsiveness and can lead to apoptosis. *Biochem Pharmacol* 2004; **68**: 409–416.

38. Kefas BA, Cai Y, Ling Z, Heimberg H, Hue L, Pipeleers D *et al*. AMP-activated protein kinase can induce apoptosis of insulin-producing MIN6 cells through stimulation of c-Jun-N-terminal kinase. *J Mol Endocrinol* 2003; **30**: 151–161.

39. Cai Y, Wang Q, Ling Z, Pipeleers D, McDermott P, Pende M *et al*. Akt activation protects pancreatic beta cells from AMPK-mediated death through stimulation of mTOR. *Biochem Pharmacol* 2008; **75**: 1981–1993.

40. Pinton P, Giorgi C, Siviero R, Zecchini E, Rizzuto R. Calcium and apoptosis: ER-mitochondria Ca2 + transfer in the control of apoptosis. *Oncogene* 2008; **27**: 6407–6418.

41. Ahn YJ, Kim H, Lim H, Lee M, Kang Y, Moon S *et al*. AMP-activated protein kinase: implications on ischemic diseases. *BMB Rep* 2012; **45**: 489–495.

42. Ravier MA, Guldenagel M, Charollais A, Gjinovci A, Caille D, Sohl G *et al*. Loss of connexin36 channels alters beta-cell coupling, islet synchronization of glucose-induced Ca2 + and insulin oscillations, and basal insulin release. *Diabetes* 2005; **54**: 1798–1807.

43. Bavamian S, Pontes H, Cancela J, Charollais A, Startchik S, Van de Ville D *et al*. The intercellular synchronization of Ca2 + oscillations evaluates Cx36-dependent coupling. *PLoS One* 2012; **7**: e41535.

44. Head WS, Orseth ML, Nunemaker CS, Satin LS, Piston DW, Benninger RK. Connexin-36 gap junctions regulate in vivo first- and second-phase insulin secretion dynamics and glucose tolerance in the conscious mouse. *Diabetes* 2012; **61**: 1700–1707.

45. Benninger RK, Zhang M, Head WS, Satin LS, Piston DW. Gap junction coupling and calcium waves in the pancreatic islet. *Biophys J* 2008; **95**: 5048–5061.

46. Tengholm A, Gylfe E. Oscillatory control of insulin secretion. *Mol Cell Endocrinol* 2009; **297**: 58–72.

47. Decrock E, Krysko DV, Vinken M, Kaczmarek A, Crispino G, Bol M *et al*. Transfer of IP(3) through gap junctions is critical, but not sufficient, for the spread of apoptosis. *Cell Death Differ* 2012; **19**: 947–957.

48. McCullough LD, Zeng Z, Li H, Landree LE, McFadden J, Ronnett GV. Pharmacological inhibition of AMP-activated protein kinase provides neuroprotection in stroke. *J Biol Chem* 2005; **280**: 20493–20502.

49. Yen JC, Chang FJ, Chang S. A new criterion for automatic multilevel thresholding. *IEEE Trans Image Proc* 1995; **4**: 370–378.

50. Moore AF, Jablonski KA, Mason CC, McAteer JB, Arakaki RF, Goldstein BJ *et al*. The association of ENPP1 K121Q with diabetes incidence is abolished by lifestyle modification in the diabetes prevention program. *J Clin Endocrinol Metab* 2009; **94**: 449–455.

51. Foretz M, Ancellin N, Andreelli F, Saintillan Y, Grondin P, Kahn A *et al*. Short-term overexpression of a constitutively active form of AMP-activated protein kinase in the liver leads to mild hypoglycemia and fatty liver. *Diabetes* 2005; **54**: 1331–1339.

52. Allagnat F, Christulia F, Ortis F, Pirot P, Lortz S, Lenzen S *et al*. Sustained production of spliced X-box binding protein 1 (XBP1) induces pancreatic beta cell dysfunction and apoptosis. *Diabetologia* 2010; **53**: 1120–1130.

Supplementary Information accompanies this paper on Cell Death and Differentiation website (http://www.nature.com/cdd)